2.1.6 Trapped lee waves

One of the most prominent features of mountain waves is the long train of wave clouds over the lee of mountain ridges in the lower atmosphere. This type of wave differs from the dispersive tails shown earlier for the $l \approx k$ case in that it is located in the lower atmosphere and there is no vertical phase tilt.

This type of trapped lee waves occur when the Scorer parameter decreases rapidly with height (Scorer 1949).

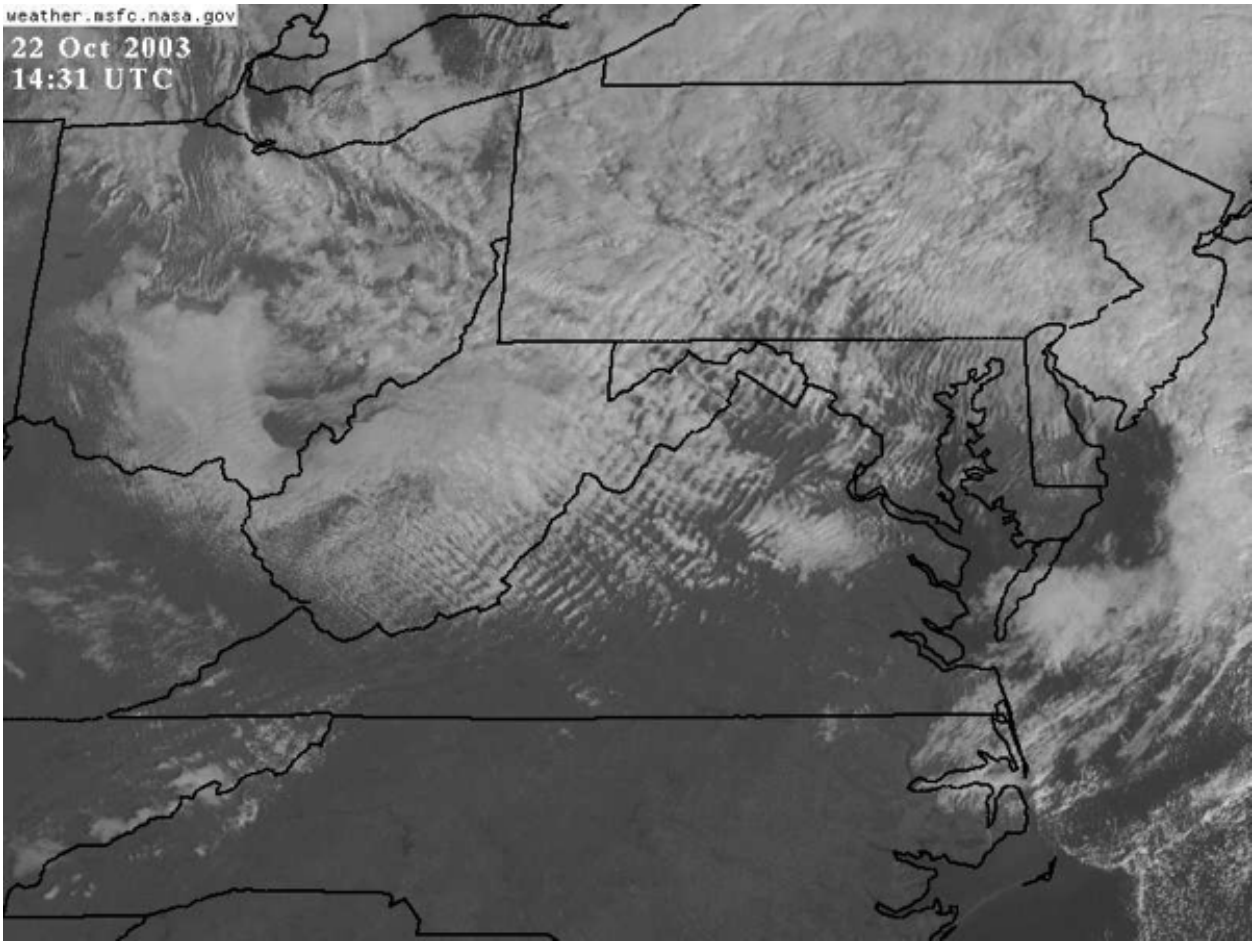

Figure 1: Satellite imagery for lee wave clouds observed at 1431 UTC, 22 October 2003, over western Virginia. Clouds originate at the Appalachian Mountains. (Courtesy of NASA).

In considering flows forced by two-dimensional sinusoidal mountains and two-dimensional isolated mountains, we made the following assumptions and approximations when constructing the equations of motion:

- steady-state ($\partial/\partial t = 0$)
- non-rotating ($f = 0$)
- adiabatic $\dot{q} = 0$
- Boussinesq (incompressible, $\nabla \vec{u} = 0$; $\rho = \overline{\rho}$, except with g)
- inviscid (F_{rx} and $F_{rz} = 0$)
- two-dimensional ($v = 0$, $\partial/\partial y = 0$)
- $\overline{u}(z) =$ constant
- $N(z) =$ constant

Here, we modify these assumptions to allow for vertical variation in either the zonal wind or static stability (*i.e.,* $\overline{u}(z)$ or $N(z) \neq$ constant). Here, the governing equation is

$$\nabla^2 w^{'} + l^2(z) w^{'} = 0 \,, \tag{1}$$

where the Scorer parameter takes its full form

$$l^2(z) = \frac{N^2(z)}{\overline{u}^2(z)} - \frac{1}{\overline{u}(z)} \frac{\partial^2 \overline{u}(z)}{\partial z^2} \,. \tag{2}$$

The condition for vertical propagation becomes $k_s < l$, where k_s is the s-th Fourier component of the topography. If the mean cross mountain wind speed increases strongly with height, or there is a low-level stable layer so that N decreases strongly with height, there may two layers of fluid with different Scorer parameter values l_U and l_L for the upper and lower layers, respectively. Assuming $l_U < l_L$, waves whose wavenumbers fall between the two Scorer parameter values will propagate vertically in the lower layer but decay with height in the upper layer. When the zonal wind or static stability are approximately constant within each layer, waves can experience refraction and/or reflection at the adjoining interface. This is physically similar to optical rays passing through fluids of varying density.

For reflection, each upward-propagating wave has an associated downward-propagating wave. The interaction of these waves is constructive (destructive) when the amplitude increases (decreases). For constructive interference, lee wave energy becomes trapped in the lower layer, which is then called a *wave duct*. The trapped wave is capable of transporting energy over long distances with little attenuation.

Linear theory is expected to reproduce accurate results when the *non-dimensional mountain height* $N h_m / \overline{u} \ll 1$. Even when this value is not necessarily small, in the cases with constant $\overline{u}$ and N, the difference between linear predictions and the full non-linear solutions remains small so long that waves do not break. However, these differences become dramatic when $\overline{u}$ and N vary in a way that produces trapped lee waves. Numerical simulations have shown that linear theory only reliably predicts wave amplitude when the ratio of lee wavelength to mountain width is greater than unity.

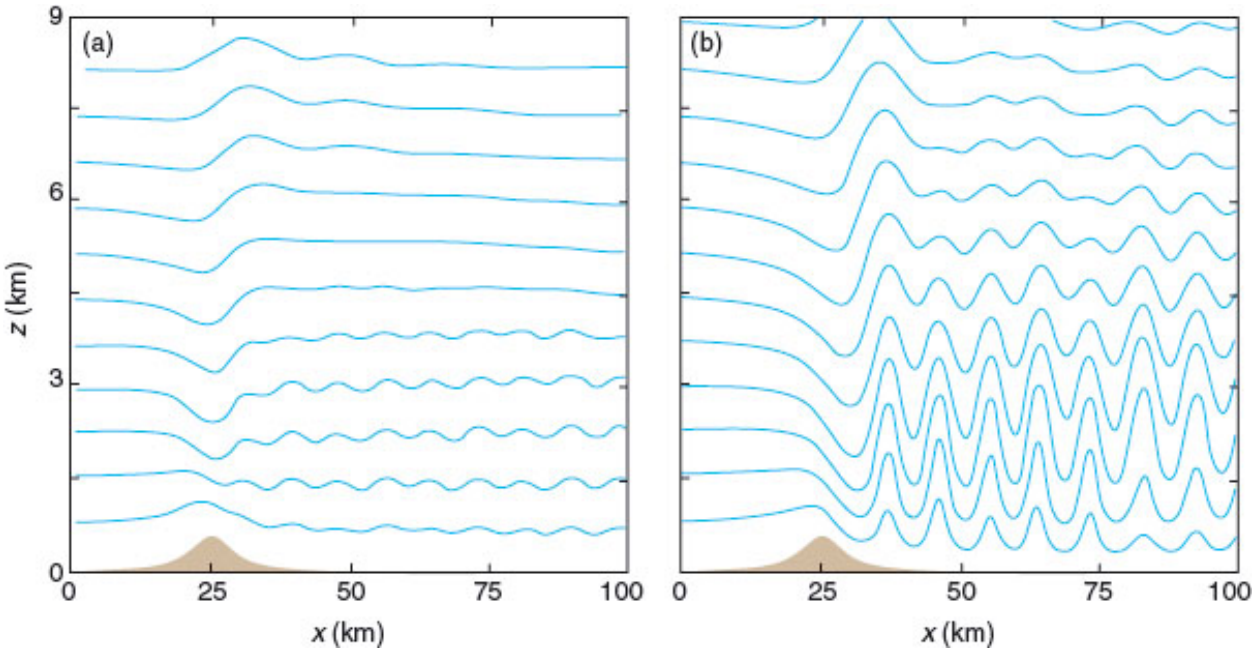

Figure 2: Streamlines in air flow over a mountain for (a) steady flow subject to the linear approximation and (b) the fully nonlinear and unsteady solution. [From Markowski and Richardson]

Lee waves and rotors

- Due to the co-existence of the upward propagating waves and downward propagating waves, there exists no phase tilt in the lee waves.
- Once lee waves form, regions of reversed cross-mountain winds near the surface beneath the crests of the lee waves may develop due to the presence of a reversed pressure gradient force.
- In the presence of surface friction, a sheet of vorticity parallel to the mountain range forms along the lee slopes, which originates in the region of high shear within the boundary layer.
- The vortex sheet separates from the surface, ascends into the crest of the first lee wave, and remains aloft as it is advected downstream by the undulating flow in the lee waves (Doyle and Durran 2004).
- The vortex with recirculated air is known as rotor and the process that forms it is known as boundary layer separation.
- These rotors are often observed to the lee of steep mountain ranges such as over the Owens Valley, California, on the eastern slope of Sierra Nevada (e.g., Grubišić and Lewis 2004).
- Occasionally, a turbulent, altocumulus cloud forms with the rotor and is referred to as rotor cloud.

2.1.7 Nonlinear flows over two-dimensional mountains

- The linear dynamics of mountain waves over 2D ridges are fundamentally understood.
- Linear theory, however, begins to break down when the perturbation velocity ($u^{'}$) becomes large compared with the basic flow ($\overline{u}$) in some regions, so that the flow becomes stagnant.
- This happens when the mountain becomes very high, the basic flow becomes very slow, or the stratification becomes very strong.
- In other words, flow becomes more nonlinear when the *Froude number*, $\overline{u}/Nh_m$, becomes small.
- For simplicity, the mountain height is denoted by h_m. Thus, in order to fully understand the dynamics of nonlinear phenomena, such as upstream blocking, wave breaking, severe downslope winds and lee vortices, we need to take a nonlinear approach.
- Nonlinear response of a continuously stratified flow over a mountain is very complicated since the nonlinearity may come from the basic flow characteristics, the mountain height, or the transient behavior of the internal flow, such as wave steepening.

Another way to understand why linear theory fails in these cases is by considering that in linear theory, the forcing at a particular wavelength is obtained by the Fourier transform of the mountain. As a result, little forcing is produced at the resonant wavelength if the mountain is much wider than that wavelength. The nonlinear wave amplitude when resonant wavelengths are short compared to the mountain width is due to enhancement of shorter wavelengths through nonlinear wave interactions rather than through direct terrain forcing. These interactions are not accounted for in linear theory.

Long (1953) derived the governing equation for the finite-amplitude, steady state, two-dimensional, inviscid, continuously and stably stratified flow and obtained an equation for vertical displacement of a streamline from its far upstream δ. It looks essentially the same as the equation for $w^{'}$ that we derived earlier for linear waves:

$$\nabla^2\delta + l^2\delta = 0\,, \tag{3}$$

where $l = N/\overline{u}$ is the Scorer parameter of the basic flow far upstream.

The main difference from the linear problem is that nonlinear lower boundary condition has to be used to represent the finite-amplitude mountain:

$$\delta(x,z) = h(x) \quad \text{at } z = h(x)\,. \tag{4}$$

The nonlinear lower boundary condition is applied on the mountain surface, instead of approximately applied at $z = 0$ as in the linear lower boundary condition. The general solution to Eq. (3) is actually similar to the linear solutions we obtained earlier.

In Fig. 6 streamlines of analytical solutions are shown for flow over a semi-circle obstacle for the non-dimensional mountain heights = 0.5, 1.0, 1.27, and 1.5. The non-dimensional mountain height (the reciprocal of the Froude number) which is a measure of the non-linearity of the continuously stratified flow.

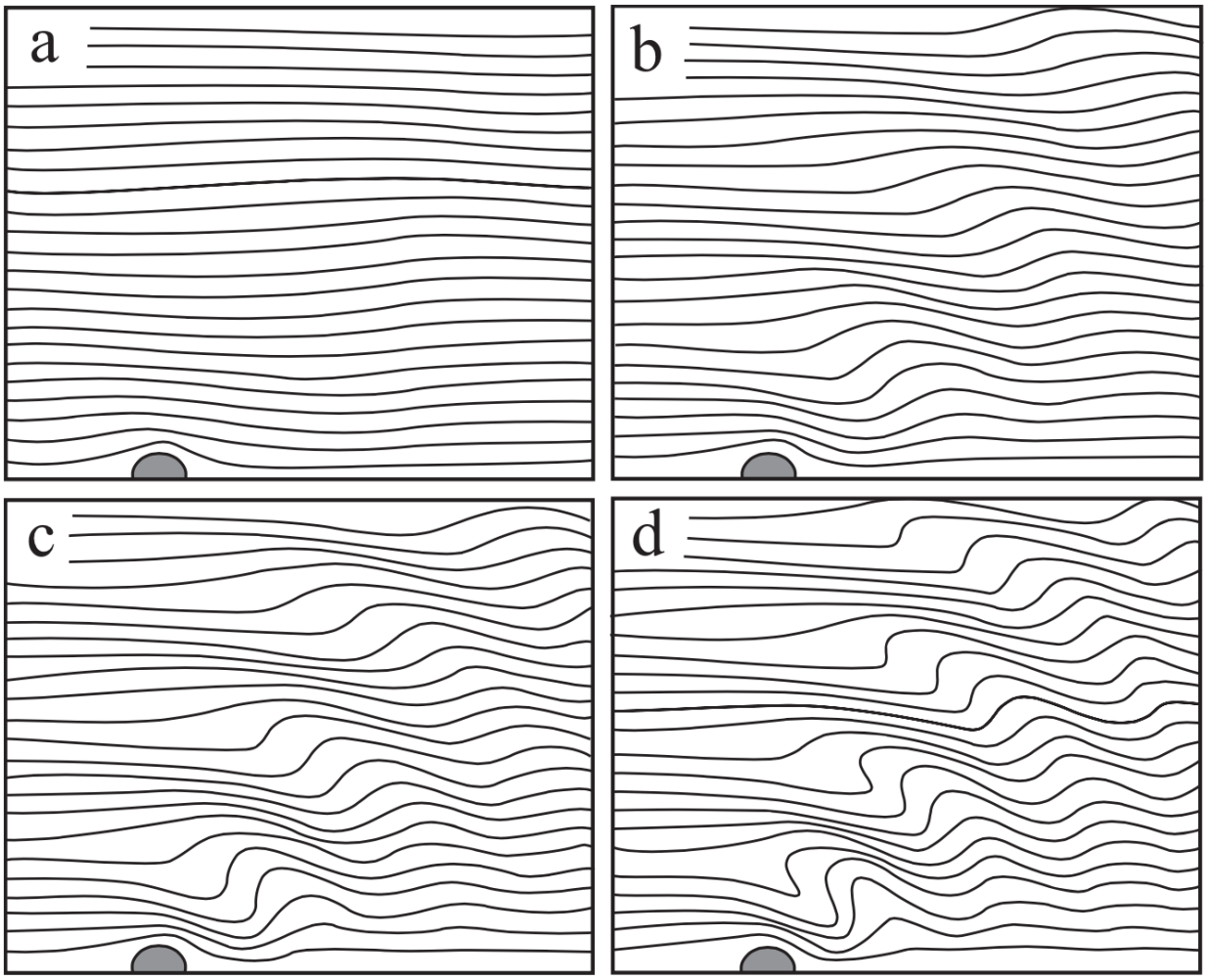

Figure 3: Streamlines of Long's model solutions for uniform flow over a semi-circle obstacle with Nh/U = (a) 0.5, (b) 1.0, (c) 1.27, and (d) 1.5. Note that the streamlines become vertical in (c) and overturn in (d). (Adapted after Miles 1968)

When $Nh_m/\overline{u}$ is small (*e.g.*, 0.5) the flow is more linear. As $Nh_m/\overline{u}$ increases to 1.27, the flow becomes more non-linear and its streamlines become vertical at the first level of wave steepening. For flow with $Nh_m/\overline{u} > 1.27$, the flow becomes statically and dynamically (shear) unstable.

2.1.8 Generation of severe downslope winds

Severe downslope winds over the lee of a mountain ridge have been observed in various places around the world, such as the *chinook* over the Rocky Mountains, *foehn* over the Alps. One well-known event is the 11 January 1972 windstorm that occurred in Boulder, Colorado. With this event, the peak wind gust reached as high as 60 ms^{-1} and produced severe damage in the Boulder, Colorado area.

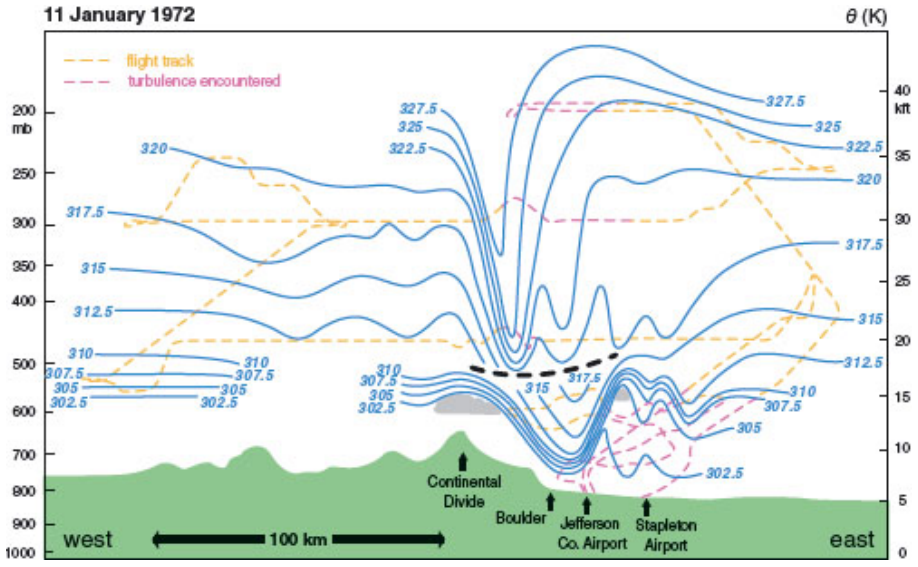

Figure 4: Analysis of potential temperatures (blue contours; K) from aircraft flight data and rawinsondes on 11 January 1972 during a downslope windstorm near Boulder, CO. [From Markowski and Richardson]

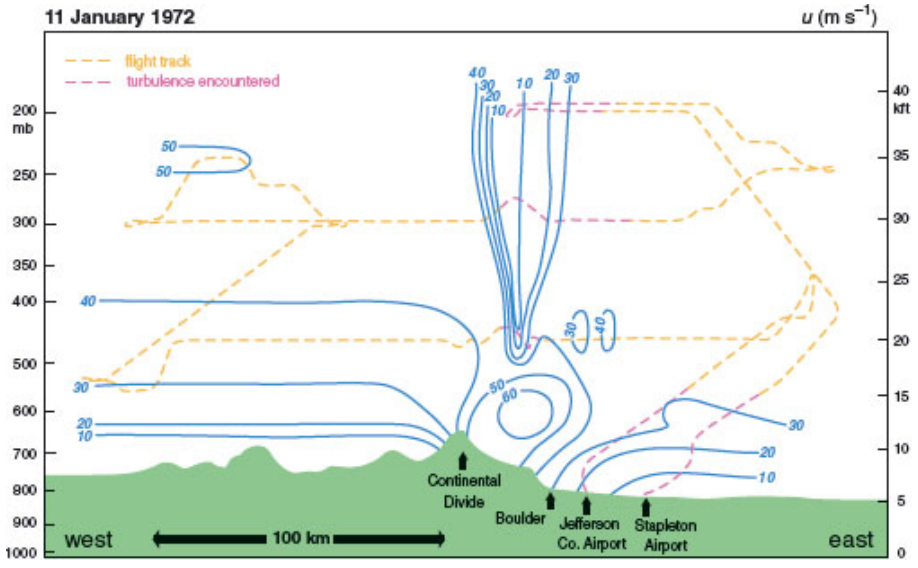

Figure 5: Analysis of the westerly wind component (blue contours; m/s) on 11 January 1972 during the downslope windstorm near Boulder, CO. [From Markowski and Richardson]

The basic dynamics of the severe downslope wind can be understood from the following two major theories: (a) *resonant amplification theory* (Clark and Peltier 1984), and (b) *hydraulic jump theory* (Smith 1985), along with later studies on the effects of instabilities, wave ducting, nonlinearity, and upstream flow blocking.

Resonant Amplification Theory

Idealized nonlinear numerical experiments indicate that a high-drag (severe-wind) state occurs after an upward propagating mountain wave breaks above a mountain.

The wave-breaking region is characterized by strong turbulent mixing, with a local wind reversal on top of it. The wind reversal level coincides with the critical level for a stationary mountain wave and, thus, is also referred to as the *wave-induced critical level*. Waves can not propagate through the critical level and are reflected downwards. The wave breaking region aloft acts as an internal boundary which reflects the upward propagating waves back to the ground and produces a high-drag state through partial resonance with the upward propagating mountain waves.

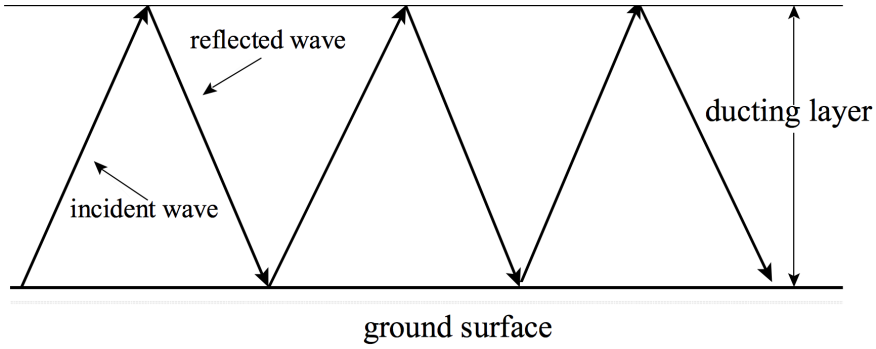

Figure 6: Illustration of wave reflection and transmission between the ground surface and some upper level. [From Nappo, 2002]

When the basic-flow critical level is located at a non-dimensional height of $z_i/\lambda_z = 3/4 + n$ (n is an integer, z_i is a prescribed critical level height, $\lambda_z = 2\pi\overline{u}/N$ is the vertical hydrostatic length scale) above the surface, non-linear resonant amplification occurs between the upward propagating waves generated by the mountain and the downward propagating waves reflected from the critical level. On the other hand, if the basic-flow critical level is located at a non-dimensional height $z_i/\lambda_z \neq 3/4 + n$ (*e.g.*, 1.15), there is no wave resonance and no severe downslope winds are generated.

Because the severe downslope winds are developed by resonance between upward and downward waves, this mechanism is referred to as the *resonant amplification mechanism*.

For the above reasons, the vertical structure of the atmosphere, particularly in terms of the Scorer parameter (as it determines the vertical wavelength), is most important for the onset of resonant response, given sufficiently strong orographic forcing to cause wave breaking. Wave breaking occurs when waves reach large enough amplitudes. When wave breaking occurs, it induces a critical level in the shear layer with low Richardson number and, thus, establishes a flow configuration favorable for wave ducting and resonant amplification in the lower uniform flow layer.

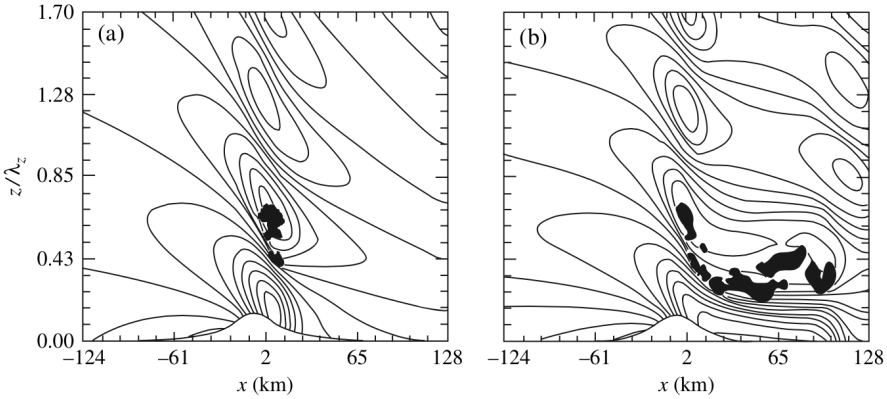

Figure 7: Wave ducting as revealed by the time evolution of horizontal wind speeds and regions of local (shaded) for a flow with uniform wind and constant static stability over a mountain ridge at (a) 12.6, and (d) 50.4. The Froude number of the uniform basic wind is 1.0. (Adapted after Wang and Lin 1999)

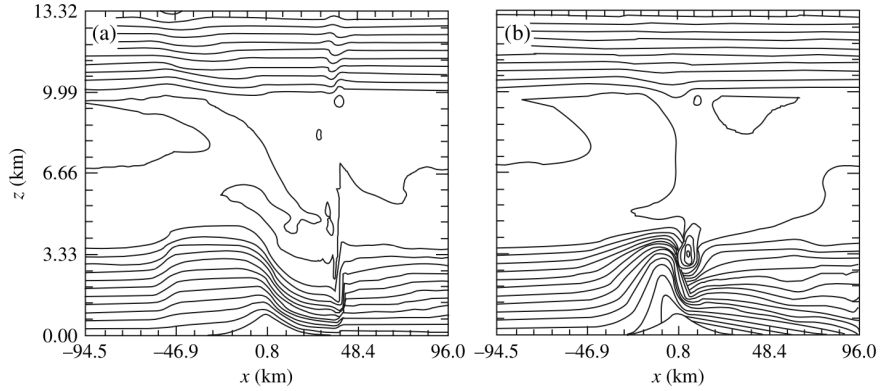

Figure 8: Effects of nonlinearity on the development of severe downslope winds: (a) Potential temperature field from nonlinear numerical simulations for a basic flow with and ; (b) Same as (a) except from linear numerical simulations. The contour interval is 1 K in both (a) and (b). (Adapted after Wang and Lin 1999)

Effects of the wave ducting on the development of high-drag states for a flow with uniform wind and constant static stability are illustrated in Fig. 7. Shortly after the occurrence of wave breaking, regions with local $Ri < 0.25$ form (Fig. 7a). This turbulent mixing region expands downward and downstream due to strong non-linear effects on the flow near the critical level (Fig. 8a). This region expands downward by wave reflection and ducting from the wave-induced critical level and accelerates downstream by the non-linear advection (Fig. 7b).

Effects of wave reflection are evidenced by the fact that the wave duct with severe downslope wind is located below the region of the turbulent mixing. In the absence of non-linearity (Fig. 8b), the wave-breaking region does not expand downward to reduce the depth of the lower uniform wind layer. This, in turn, prohibits the formation of the severe downslope wind and internal hydraulic jump.

Hydraulic Jump Theory

The above image depicts a hydraulic jump in a kitchen sink, which shows a very rapid change in the flow depth across the jump. Around the place where the tap water hits the sink, you will see a smooth looking flow pattern. A little further away, you will see a sudden 'jump' in the water level. This is a hydraulic jump.

A hydraulic theory was proposed to explain the development of severe downslope winds based on the similarity of flow configurations of severe downslope windstorms and finite-depth, homogeneous flow over a mountain ridge (Smith 1985).

The hydraulic theory attributes the high-drag (severe-wind) state to the interaction between a smoothly stratified flow and the deep, well-mixed, turbulent "dead" region above the lee slope in the middle troposphere.

Though not directly applicable to stratified atmosphere associated with downslope wind storms, using shallow water theory will offer some intuition about flow traversing a barrier.

Assume there is a layer of fluid with density ρ, where the top of the layer is a free surface. The terrain height is h_t and the perturbation fluid depth is D, such that the height of the free surface is $D + h_t$ (Fig. 9).

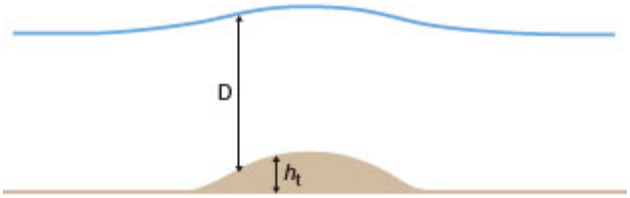

Figure 9: Relationship between free surface height, depth (D), and terrain height (h_t).

The boundary conditions are given by

$$w(x, h_t) = u\frac{\partial h_t}{\partial x} \tag{5}$$

$$w(x, D + h_t) \approx u\frac{\partial (D + h_t)}{\partial x}\,. \tag{6}$$

Now, we consider the equations of motion for non-linear, steady-state, inviscid, hydrostatic fluid in a non-rotating reference frame

$$u\frac{\partial u}{\partial x} + \frac{1}{\rho}\frac{\partial p}{\partial x} = 0 \tag{7}$$

$$\frac{\partial u}{\partial x} + \frac{\partial w}{\partial z} = 0 \tag{8}$$

To make things more convenient, we want to eliminate p and w in favor of D and h_t so that the flow accelerations following a parcel can be related to changes in the depth of the fluid and to the slope of the terrain. Assuming hydrostatic balance, $\partial p = -\rho g \partial z$, which leads to

$$\frac{1}{\rho}\frac{\partial p}{\partial z} = -g\frac{\partial (D + h_t)}{\partial x}.$$

The continuity equation can be integrated with respect to z over the fluid depth to obtain

$$\int_{h_t}^{D+h_t} \frac{\partial u}{\partial x} dz + \int_{h_t}^{D+h_t} \frac{\partial w}{\partial z} dz = 0$$

$$\frac{\partial u}{\partial x}(D + h_t - h_t) + w(D + h_t) - w(h_t) = 0$$

$$\frac{\partial u}{\partial x} D + u\frac{\partial (D + h_t)}{\partial x} - u\frac{\partial h_t}{\partial x} = 0\,.$$

Note that $\partial u/\partial x$ was pulled outside of the integral because u is independent of z for all times if it is initially. Eq. (7) suggests that u depends on the horizontal pressure gradient force, which itself only depends on the fluid depth (independent of z). Thus, the equations of motion can be rewritten as

$$u\frac{\partial u}{\partial x} + g\frac{\partial D}{\partial x} = -g\frac{\partial h_t}{\partial x} \tag{9}$$

$$\frac{\partial (uD)}{\partial x} = 0\,. \tag{10}$$

Equation (9) states that a steady-state is achieved through a balance between horizontal advection and horizontal pressure gradient force. Equation (10) states that mass is conserved by requiring a constant mass flux in the x-direction. Constant mass flux means that a thickening (thinning) of the fluid is associated with deceleration (acceleration) following the particle.

We now seek to combine Eqs. (9) and (10) into a single equation. To do this, we solve for $\partial u/\partial x$ in Eq. (10) and substitute the result into Eq.(9). This yields

$$-\frac{u^2}{D}\frac{\partial D}{\partial x} + g\frac{\partial D}{\partial x} = -g\frac{\partial h_t}{\partial x}\,. \tag{11}$$

Divide by g to obtain

$$\left(1 - \frac{u^2}{gD}\right)\frac{\partial D}{\partial x} = -\frac{\partial h_t}{\partial x}\,. \tag{12}$$

The intrinsic shallow-water gravity wave speed is defined as $c^2 \equiv gD$. Substitution into Eq. (12) yields

$$\left(1 - \frac{u^2}{c^2}\right)\frac{\partial D}{\partial x} = -\frac{\partial h_t}{\partial x}\,, \tag{13}$$

which is equivalent to

$$\left(1 - \mathrm{Fr}^2\right)\frac{\partial D}{\partial x} = -\frac{\partial h_t}{\partial x}\,, \tag{14}$$

where $\mathrm{Fr} = u^2/c^2$ is the *Froude number* for shallow-water theory. Here, the Froude number is the ratio of the mean flow to the gravity wave phase speed.

When $\mathrm{Fr} > 1$, gravity waves are unable to propagate upstream relative to the mean flow, and the fluid is unable to produce perturbation pressure gradients of sufficient magnitude to balance nonlinear advection.

We will now use this Froude number to identify three distinct flow regimes.

Fr $>$ 1

Based on Eq. (14), if Fr > 1 and $\partial h_t/\partial x > 0$, then $\partial D/\partial x > 0$. This means that fluid traveling uphill will thicken, reaching its maximum thickness at the peak of the mountain (Fig. 10a). Conversely, on the lee side, $\partial h_t/\partial x < 0$ and $\partial D/\partial x < 0$, meaning that the fluid thins. As the thickness of the fluid changes, the zonal velocity also changes in accordance with the constant zonal mass flux prescribed by the continuity equation. Thus, when Fr > 1, there is a minimum in zonal velocity at the top of the mountain where the fluid is thickest.

If we consider a parcel embedded in a westerly wind, the parcel will decelerate as it passes over the mountain and then return to its original wind speed at the leeward base of the mountain (assuming we neglect friction). This regime represents a transfer of energy from kinetic to potential and back to kinetic. We find such behavior to be quite intuitive. Consider, for example, a ball rolling up a hill then descending once it crests the peak. Flow where Fr > 1 is called *supercritical flow*.

Fr $<$ 1

Based on Eq. (14), if Fr < 1 and $\partial h_t/\partial x > 0$, then $\partial D/\partial x < 0$. This means that fluid traveling uphill will thin, reaching its maximum thinness at the peak of the mountain (Fig. 10b). Conversely, on the lee side, $\partial h_t/\partial x < 0$ and $\partial D/\partial x > 0$, meaning that the fluid thickens. The behavior associated with subcritical flow as a parcel traverses a mountain is not in line with our usual arguments regarding the simple transfer of energy from kinetic to potential, and we must break with our conceptual model of an isolated ball rolling up a hill.

An air parcel feel the presence of surrounding air parcels through the pressure gradient force. Thus, the acceleration obtained by an isolated air parcel depends on the difference between the pressure gradient force arising from changes in the fluid depth (the second term in Eq. 9) versus the amount of work (*i.e.*, conversion of kinetic energy to potential energy) associated with ascending the terrain. Here, the pressure gradient force dominates and leads to a net positive acceleration following the parcel as it ascends. On the lee side, the fluid thickens and returns to its original depth as the parcel decelerates to its original speed. Flow where Fr < 1 is called *subcritical flow*.

Fr $\approx$ 1 (initially)

Both of the previously considered cases both return the parcel to its original wind speed when it reaches the lee side. How do we get winds that accelerate along the entire path from the windward to the leeward side? For the windward side, this acceleration requires subcritical flow, while on the leeward side the acceleration requires supercritical flow. In other words, the acceleration on the windward side must cause u to cross the threshold from subcritical to supercritical flow, which is likely to happen only if the flow has a Fr close to unity at the start.

The transition from subcritical to supercritical results in leeward wind speeds that exceed their original value on the windward side. In accordance with the increasing speeds, the fluid thickness decreases over the entire path. This causes the free surface to drop sharply on the leeward side (analogous to the descending isentropes during downslope wind events) and results in what is called a hydraulic jump. Hydraulic jumps are very turbulent, and large amounts of energy are dissipated within them.

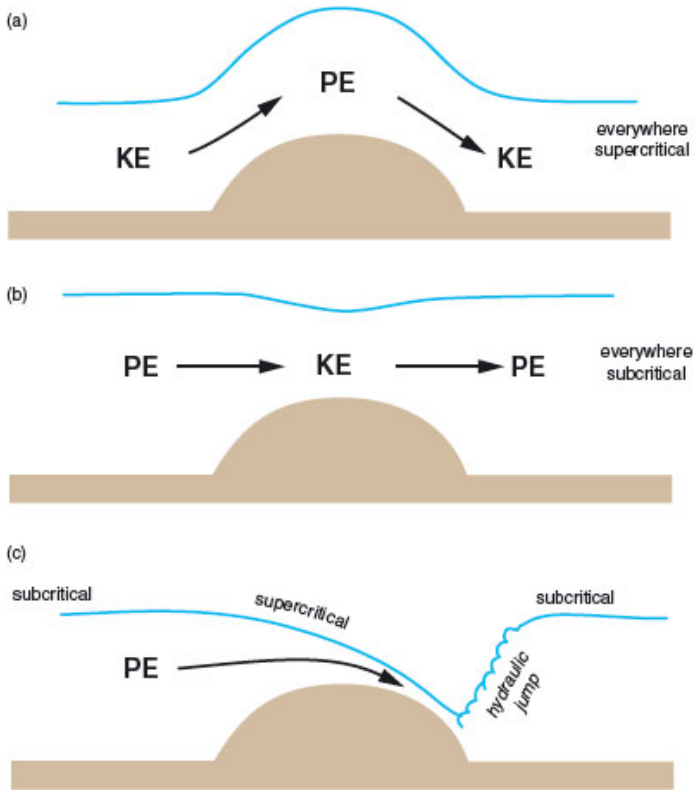

Figure 10: Flow over an obstacle for the simple case of a single layer of fluid having a free surface. (a) Supercritical flow (Fr > 1) everywhere, (b) Subcritical flow (Fr < 1) everywhere, (c) Supercritical flow on the lee slope with adjustment to subcritical flow at a hydraulic jump near the base of the obstacle. [From Markowski and Richardson])

Predicting downslope wind storms

Putting all of this together, here are some of the conditions that forecasters look for when predicting downslope windstorms:

- an asymmetric mountain with a gentle windward slope and a steep lee slope
- strong cross-mountain geostrophic winds ($> 15\ \mathrm{ms}^{-1}$) at and just above mountain-top level associated with surface high pressure upstream and surface low pressure downstream
- an angle between the cross-mountain flow and the ridge that is greater than $\sim 60\,\mathrm{deg}$
- a stable layer near or just above the mountain top, and a layer of lesser stability above
- a level that exhibits a wind direction reversal or where the cross-barrier flow simply goes to zero (the mean state critical level); the existence of weak, vertical wind shear or reverse shear is more favorable than forward shear
- situations of cold advection and anticyclonic vorticity advection, which promote downward synoptic motion to generate and reinforce the vertical stability structure
- absence of a deep, cold, stable layer in the lee of mountains, which may keep the downslope flow from penetrating to the surface.

2.1.9 Trapped Lee Waves Behind a 3D Mountain

Although the two-dimensional mountain wave theories helped explain some important flow phenomena generated by infinitely long ridges, such as upward propagating mountains waves, lee waves, wave overturning and breaking, and severe downslope winds, in reality most of the mountains are of three-dimensional, complex form.

As in the two-dimensional mountain wave problem, a rapid decrease of the Scorer parameter with height leads to the formation of trapped lee waves. The formation of three-dimensional trapped lee waves is similar to that of *Kelvin ship waves* over the water surface.

Figure 11 is an example of the cloud streets associated with three-dimensional trapped lee waves produced by flow past a mountainous island. The wave pattern is generally contained within a wedge with the apex at the mountain.

Figure 11: Satellite imagery showing three-dimensional trapped lee waves induced by the Sandwich Islands in southern Atlantic Ocean on November 23, 2009. The wave pattern is similar to that of the ship waves. (credit: NASA)

The three-dimensional trapped lee waves are composed by *transverse waves* and *diverging waves*. The transverse waves lie approximately perpendicular to the flow direction, and are formed by waves attempting to propagate against the basic flow but that have been advected to the lee.

The formation mechanism of transverse waves is the same as that of the two-dimensional trapped lee waves. Unlike the transverse waves, the diverging waves attempt to propagate laterally away from the mountain and have been advected to the lee.

Also, the diverging waves have crests that meet the incoming flow at a rather shallow angle. Both of the transverse and diverging waves are mathematically associated with a stationary phase point, and the significant disturbance is confined within a wedge angle of about $19°28'$ with the x-axis.

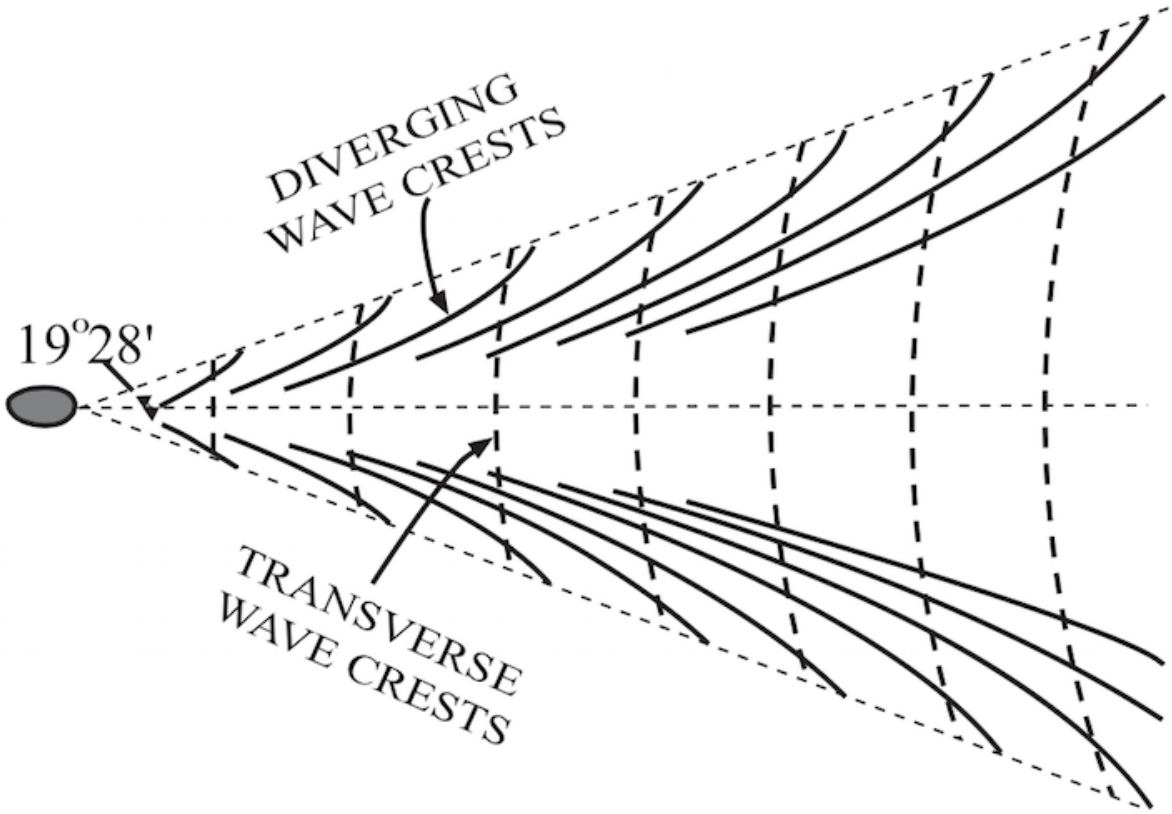

Figure 12: Schematic of transverse (bold-dashed) and diverging (solid) phase lines for a classical deep water ship wave. (Adapted after Sharman and Wurtele 1983)